Evaluating Critical Uncertainty Thresholds in a Spatial Model of Forest Pest Invasion Risk

Frank H. Koch,[1] Denys Yemshanov,[2]* Daniel W. McKenney,[2] and William D. Smith[3]

Pest risk maps can provide useful decision support in invasive species management, but most do not adequately consider the uncertainty associated with predicted risk values. This study explores how increased uncertainty in a risk model's numeric assumptions might affect the resultant risk map. We used a spatial stochastic model, integrating components for entry, establishment, and spread, to estimate the risks of invasion and their variation across a two-dimensional landscape for *Sirex noctilio*, a nonnative woodwasp recently detected in the United States and Canada. Here, we present a sensitivity analysis of the mapped risk estimates to variation in key model parameters. The tested parameter values were sampled from symmetric uniform distributions defined by a series of nested bounds ($\pm 5\%, \ldots, \pm 40\%$) around the parameters' initial values. The results suggest that the maximum annual spread distance, which governs long-distance dispersal, was by far the most sensitive parameter. At $\pm 15\%$ or larger variability bound increments for this parameter, there were noteworthy shifts in map risk values, but no other parameter had a major effect, even at wider bounds of variation. The methodology presented here is generic and can be used to assess the impact of uncertainties on the stability of pest risk maps as well as to identify geographic areas for which management decisions can be made confidently, regardless of uncertainty.

KEY WORDS: Invasive species; parametric uncertainty; pest risk mapping; stochastic modeling; sensitivity analysis

1. INTRODUCTION

Invasive alien species have caused significant deleterious impacts on the agriculture, forestry,

[1] Department of Forestry and Environmental Resources, North Carolina State University, Raleigh, NC, USA, and Forest Health Monitoring Program, USDA Forest Service, Research Triangle Park, NC 27709, USA.
[2] Natural Resources Canada, Canadian Forest Service, Great Lakes Forestry Centre, Sault Ste. Marie, Ontario P6A 2E5, Canada.
[3] Southern Research Station, USDA Forest Service, Research Triangle Park, NC 27709, USA.
* Address correspondence to Denys Yemshanov, Natural Resources Canada, Canadian Forest Service, Great Lakes Forestry Centre, 1219 Queen Street East, Sault Ste. Marie, Ontario P6A 2E5, Canada; tel: 705-541-5602; fax: 705-541-5700; dyemshan@nrcan.gc.ca.

and public health sectors, with worldwide economic losses estimated at US$1.4 trillion annually, or roughly 5% of the global economy.[1] Since species introductions are strongly linked to global trade, this level of impact is likely to persist into at least the near future.[2,3] Notably, such substantial economic losses are caused by the small number of invasive alien species that actually survive beyond introduction and become established in new geographic areas.[4] These survivors may subsequently disrupt native ecosystems and communities[4–6] and imperil native species through predation or competition.[7,8]

Assessing the level of invasion risk and potential impact posed by organisms of interest is a critical initial stage in a systematic response to emerging invasive alien species threats. While regulatory agencies commonly issue risk assessments for newly

recognized pests, the models underlying these risk assessments are rarely quantitative because of a dearth of scientific data for many pests and are usually limited to a simplified characterization of establishment or impact potential.[9–11] As a result, the historical emphasis in invasive alien species risk management has been on preventing introductions rather than on the development of comprehensive response strategies for all potentially impacted geographic areas; thus, spatial aspects of risk have often been neglected,[12,13] even though total risk of both invasion and impact clearly varies between geographic domains.[14] Nevertheless, risk maps, as the spatially explicit realizations of risk assessments, have become increasingly popular among decisionmakers and regulators as support tools to allocate resources for quarantine, monitoring, and control of invasive alien species.[9,15]

1.1. Uncertainty in Risk Estimates of Invasion

Uncertainties are intrinsic to all risk analyses. Unfortunately, public calls for action when a new invasive organism is detected in a given area seldom allow enough time to acquire the necessary scientific knowledge to characterize the potential risk well, so uncertainty becomes an inherent feature of the analysis.[16] Systematic characterization of uncertainty is complicated by the fact that there are different definitions of the types as well as the potential sources of uncertainty.[16–21] In general terms, uncertainty may be categorized as stochastic (associated with natural variability) or epistemic (derived from incomplete knowledge about the system of interest). Stochastic uncertainty is irreducible but may be represented in a formal manner (e.g., as a probability distribution), while epistemic uncertainty can, in theory, be reduced through additional research or data.[18,19] With respect to models, uncertainties associated with parameter values or functions (parametric uncertainty hereafter) or with input data (input uncertainty) propagate to uncertainty in the model output.[21,22] Some of the inputs and parameters may be correlated or otherwise interact.[23,24] The model formulation or structure, and even its particular software implementation,[21] may also contribute to the output uncertainty.

Recently, there has been much literature discussing the characterization of uncertainty in general and ecological risk analysis[14,17,20,21,24,25] as well as in specific invasive alien species contexts.[5,26,27] Similarly, Li and Wu[22] provided an overview of un-

certainty analysis methods for large-scale ecological models used as environmental decision support. The relevance of uncertainty when characterizing complex ecological phenomena is thus widely acknowledged, but in practice, analysts often overlook (or only partially acknowledge) uncertainty and present their results as effectively certain.[16,18,20,22] Although uncertainty can lead to erroneous decisions and overconfidence, its quantification is frequently seen as too complex or time-consuming.[16,24,26]

Poor characterization of uncertainty is a particular flaw of many risk maps for invasive alien species. Most current mapping analyses involve the use of geographic information systems (GIS) software. While there may be substantial analytical capacity to quantify uncertainty in GIS applications,[28–30] most GIS software packages still do not have good methods for representing uncertainty, and so it is easy for typical GIS users to create elegant but fundamentally flawed results.[31] Moreover, published studies on uncertainty analysis in GIS have focused primarily on the propagation of spatial uncertainties; uncertainty analysis in dynamic (i.e., temporal as well as spatial) GIS models is a still-developing field of inquiry.[32] Conversely, many conceptual approaches for characterizing uncertainty in risk analysis, such as imprecise probability theory,[17] fuzzy/rough set theory,[33,34] and info-gap theory,[35,36] have been rarely implemented in a spatial context. A special challenge for risk maps is that their reliability in the face of uncertainty may be judged at multiple scales: the entire map, particular regions, or perhaps most critically, for individual and sometimes very specific geographic locations.

1.2. Objectives

In previous work,[37] we modeled the potential invasion of a recently detected woodwasp species, *Sirex noctilio* Fabricius, in eastern North American forests. Native to Europe, western Asia, and northern Africa, *S. noctilio* has been introduced in many locations throughout the world and is considered to be a significant pest of pine plantations (*Pinus* sp.) in the Southern Hemisphere.[38,39] Given the insect's high bioclimatic tolerance,[38] *S. noctilio* had been considered a major threat to North America for some time before it was discovered in upstate New York in 2004[40] and southern Ontario in 2005.[41]

In this prior analysis,[37] we generated risk maps for *S. noctilio* using a spatial stochastic model that integrates the entry, establishment, and spread

components of an invasion into a single framework. Adopting an approach of repeated stochastic model simulations, we quantified the risk of *S. noctilio* invasion as a probabilistic estimate[42,43] for each geographic location (map cell) comprising the study area. The approach also allowed us to calculate the variation of risk estimates in each cell, as propagated from the model's numeric assumptions. This methodology allowed us to estimate both risks and associated uncertainties of *S. noctilio* invasion.

Subsequently, we had three primary objectives for the follow-up study presented in this article. The first was to estimate the influence of variation in key model parameters on the predictions of invasion risk and their associated levels of uncertainty. This type of sensitivity analysis (i.e., the relative influence of changes to various input and/or parameter values on the model outputs) and uncertainty analysis (propagation of uncertainty from inputs to outputs) is common across disciplines[22,24,30,44] and, in particular, in testing the stability of ecological models.[36] Our second objective was to find the levels of introduced parametric uncertainty that would dramatically change the output maps and affect their utility as decision support tools. Notably, some portions of a risk map may remain stable even if substantial parametric variation is introduced to the model. Hence, our third objective was to identify any geographic areas where the risk map remains stable enough for decisionmakers to use it confidently in planning responses to *S. noctilio* invasion.

2. METHODS

We used the Canadian Forest Service Forest Bioeconomic Model (CFS-FBM) to perform the spatial simulations for this study. The CFS-FBM is a spatially explicit, raster-based framework that integrates biophysical and economic components. While it includes, for example, components for modeling wood supply impacts and bioeconomics of carbon sequestration,[45,46] we used it only to generate risk maps of *S. noctilio* invasion in eastern North America. As a dynamic spatiotemporal model,[47,48] the CFS-FBM has an important advantage over static risk modeling approaches, which typically adopt the simplifying assumption that an invader's potential distribution is already at an equilibrium state.[26] The model components used for risk mapping were described previously,[37] so here we provide only brief descriptions of the relevant components, primarily

to highlight the model parameters for which sensitivity/uncertainty analyses were performed. For the ease of comparison, we have employed the same notation as in our earlier study.

2.1. Entry

The CFS-FBM depicts potential introductions of a pest into an area of interest as well as the expansion of already established populations. With respect to introductions, the U.S. Department of Agriculture (USDA) Animal and Plant Health Inspection Service (APHIS) Port Information Network (PIN) database (see Haack[49] for a description) reports that *S. noctilio* has only been intercepted at U.S. marine ports of entry (i.e., not at airports or border crossings). Hence, we used the CFS-FBM to simulate new entries of *S. noctilio* at U.S. and Canadian marine port locations. Like many other forest pests,[49,50] *S. noctilio* has been linked to either commodities shipped with solid wood packing materials or raw wood products. Our calculation of *S. noctilio* entry probabilities at marine ports involved two steps:[51] estimation of the "global" entry potential and apportionment of this value among all port locations. The global entry potential is the annual probability of successful new *S. noctilio* introduction for the entire study. We estimated this probability based on the dynamics of total annual imports to the United States and Canada[52,53] from 1970 to 2006; for example, the global entry potential in 2006 was calculated as 0.172 (see prior study[37] for additional details). With respect to later years, we assumed that the global entry potential would drop in 2007 by 50% as a result of the adoption of recent international phytosanitary wood treatment standards[54] and then grow by 7% per year thereafter. This scenario thus anticipates relatively modest long-term impacts of the new standards, as implemented by both the United States and Canada in 2006, and is equivalent to a "high-risk" scenario outlined in our previous study.[37]

We apportioned the global entry potential among all ports of entry using a vector of local entry probabilities, $W_{x(t)}$, for each port x at each year t. The probabilities for individual ports were calculated from the relative tonnages of *S. noctilio*-associated commodities (based on the PIN database) received annually at the ports, as determined from marine import data for the United States and Canada.[55–60] These values (i.e., the probabilities of *S. noctilio*

establishment at the ports' locations) were used to generate entry events into eastern North America through time.[43]

2.2. Spread and Establishment

For biological realism, spread was represented as a coalescing colony using the traveling wave model of Sharov and Liebhold.[61] In our case, the rate of metapopulation expansion for any given map cell was modeled as a function of the distance between it and the other nearest cell where *S. noctilio* was already established. Since few data were available regarding the pest's behavior in North America,[38,62] the shape of this function was based on expert estimates.[37,45] In addition to the distance from the nearest already infested cell, there are two other key parameters in the spread function: p_0, the probability of colonization in the nearest adjacent map location (i.e., the local infestation probability); and d_{max}, the maximum distance from an already infested location at which a new cell may be successfully invaded (i.e., a long-distance dispersal constraint). For *S. noctilio*, d_{max} was set to 50 km and p_0 to 0.2.

The model also tracked the maximum population growth of *S. noctilio* in order to estimate the projected amount of host mortality and the establishment potential. In a cell successfully invaded by *S. noctilio*, the maximum population size is constrained by a carrying capacity, k, that is reached by geometric growth at a constant annual rate, R:[61]

$$N_{j(t+1)} = RN_{j(t)} \forall N_{j(t+1)} < k \quad \text{and}$$
$$N_{j(t+1)} = k \forall N_{j(t+1)} \geq k, \tag{1}$$

where T is the time since initial infestation, and $N_{j(t)}$ and $N_{j(t+1)}$ are the population densities at years t and $t + 1$. Essentially, k limits the maximum volume of pine killed by *S. noctilio* at time t, $\lambda_{j(t)}$, depending on the minimum volume of pine required to support a single population unit, μ:

$$\lambda_{j(t)} = \mu N_{j(t)} \forall N_{j(t)} < k \quad \text{and}$$
$$\lambda_{j(t)} = \mu k \forall N_{j(t)} = k. \tag{2}$$

Because the *S. noctilio* population density in a map cell at any given time t may be limited by the amount of currently available (i.e., unconsumed) host resource (such that $N_{j(t)} \leq \lambda_{j(t)}/\mu$), the carrying capacity can thus be viewed as a constraint that sets the annual limit for host mortality, which in turn affects the establishment potential.

The probability that an *S. noctilio* population will become successfully established in an invaded location also depends on the susceptibility of the available pine hosts. Host susceptibility, s_v, was defined as a species-dependent function of stand age (i.e., the average stand age in a map cell). A cell's s_v value equates to the probability of successful establishment in the cell, but also serves as a modifier for determining what proportion of pines in the cell are susceptible to *S. noctilio*. The s_v value is set to 0 when the stand age is less than the typical age of stand closure for pines (20 years) and is maximized when the stand age exceeds 65 years; notably, we employed different maximum susceptibility values for two pine groups, high- and low-hazard, based on the USDA Forest Service susceptibility ratings.[63]

Maps of the stand volume of pine species in our study area were derived from the National Forest Inventory for Canada[64] and the USDA Forest Service Forest Inventory and Analysis Database.[65] Individual species maps were aggregated into the high- and low-hazard pine groups. The amount of pine host resource in these groups was modeled with growth rates, g_v, based on normal yield curves constructed for the Canadian[66] and U.S.[67] portions of our study area (see prior study[37] for details). The yield curves were also used to estimate the amount of host surviving after *S. noctilio* infestation.

2.3. Mapping Risk and Output Uncertainty

Our "baseline scenario" simulates *S. noctilio* spread across eastern North America from currently known locations and potential new entries at U.S. and Canadian ports over a 30-year time horizon. (As noted in Section 2.1, this baseline scenario is equivalent to a "high-risk" scenario presented in our previous study.[37]) We initialized the model with the 2006 map of known *S. noctilio* infestations identified by field surveys in the United States and Canada. Our output map resolution was 5 × 5 km². Following our earlier work,[37] we define invasion risk for any given map cell i as the probability, p, that *S. noctilio* invades a minimum area equal to the size of a map cell at the end of the forecast horizon. The value of p for each cell was calculated through repetitive model simulations:

$$p = \frac{\sum_{n=1}^{N_{obs}} \tau_{i,n,T}}{N_{obs}}, \tag{3}$$

where $\tau_{i,n,T}$ is a binary variable indicating the presence or absence of *S. noctilio* in cell i at time horizon T for a single model replication n, and N_{obs} is the number of replications. The variation of p values (i.e., the output uncertainty) was characterized with a map of the standard deviations of p, $\sigma(p)$.

Complex stochastic simulation models usually require a sizeable number of replications to achieve stability of the outputs.[24,43] We evaluated the minimum number of model replications required to stabilize the maps of p and $\sigma(p)$ (see the related discussion of convergence for the sensitivity analysis scenarios in Section 2.4). Our previous work[37] suggested three useful convergence metrics: square root of the total map area with $p < 0.1$, square root of the map area with $\sigma(p) < 0.2$, and S_{XY}, the sum of the squared differences in p map values between two trials incorporating consecutively increasing numbers of replications:

$$S_{XY} = \sqrt{\sum_{i=1}^{M}[(p_{iX} - p_{iY})^2]}, \quad (4)$$

where M is the total number of map cells covering eastern North America ($\sim$156,000) and p_{iX} and p_{iY} are the invasion probabilities for map cell i in trials using X and Y number of replications, where $X > Y$.

2.4. Sensitivity Analysis

We analyzed the sensitivity of the invasion risk estimates to variation in several key model parameters using four common steps: (1) generating a probability distribution associated with a parameter of interest, (2) sampling from this distribution to select a value, (3) performing multiple simulations of the risk model with the parameter values sampled from the distributions, and (4) summarizing the results from repeated realizations of this process.[22,24,29,30] A parameter or input may be poorly known or specified, so its associated distribution may have to be approximated; in such cases, perhaps the simplest approach is to assume a uniform distribution.[24,68] For this study, we used a nested set of variability bounds around each tested parameter: $\pm 5\%$, $\pm 10\%$, and so on up to $\pm 50\%$. Each pair of "plus-minus" bounds defined the endpoints for a symmetric uniform distribution from which we sampled values randomly for input into the model. Importantly, the mean values of the uniform distributions remained unchanged and matched the baseline parameter values.

We identified six parameters that we believe are key drivers of the model: $W_{x(t)}$, the annual probabilities of new local entries of *S. noctilio* at individual U.S. and Canadian ports; k, the *S. noctilio* population carrying capacity at a given location (k also sets the maximum rate of host mortality); d_{max}, the maximum annual spread distance; p_0, the probability of invasion at the nearest cell adjacent to a given infested location; s_v, susceptibility of the host resource; and g_v, growth rate of the host trees (all parameters were described previously). At each variability level, we varied values for one parameter at a time, leaving the other parameters unchanged (i.e., local sensitivity analysis). To verify the relative impact of specific parameters, we also tested an alternative approach of varying all parameters but one, which was kept at the baseline.[19,69]

Because each model simulation used independent parameter randomizations, a significant number of replications was required to stabilize the configuration of risk maps. We examined the convergence of risk maps for each of the sensitivity scenarios by generating a series of trial risk maps and then plotting the stabilization metric values (see Section 2.3) against the number of model replications. Most of the sensitivity scenarios converged after 2,400–2,700 replications (Fig. 1). (The baseline scenario did not use the parameter randomizations, so it converged after <500 replications.) Hence, we generated maps of p and $\sigma(p)$ based on 3,000 model replications for each scenario.

We also used the S_{XY} equation (Equation (4)) to compare the maps of invasion risks and their standard deviations, p and $\sigma(p)$, for each sensitivity scenario, X, with the corresponding maps from the baseline scenario, Y. The parameter S_{XY} in this case depicts cumulative changes in the risk map as a result of the introduction of parametric uncertainty. We cross-tabulated these S_{XY} differences for eastern North America as well as for three regions: eastern Canada, the northeastern United States, and the southeastern United States (Virginia, Kentucky, and all states further south in the study area). To geographically assess the impact of added parametric uncertainty on the output uncertainty of the risk maps (i.e., the $\sigma(p)$ values), we calculated "uncertainty ratios" under each scenario and mapped the results. For a map cell, the uncertainty ratio is the value of $\sigma(p)$ for the sensitivity scenario of interest divided by $\sigma(p)$ for the baseline scenario. An uncertainty ratio value is close to 1.0 when adding variation to the parameter value does not change the variability
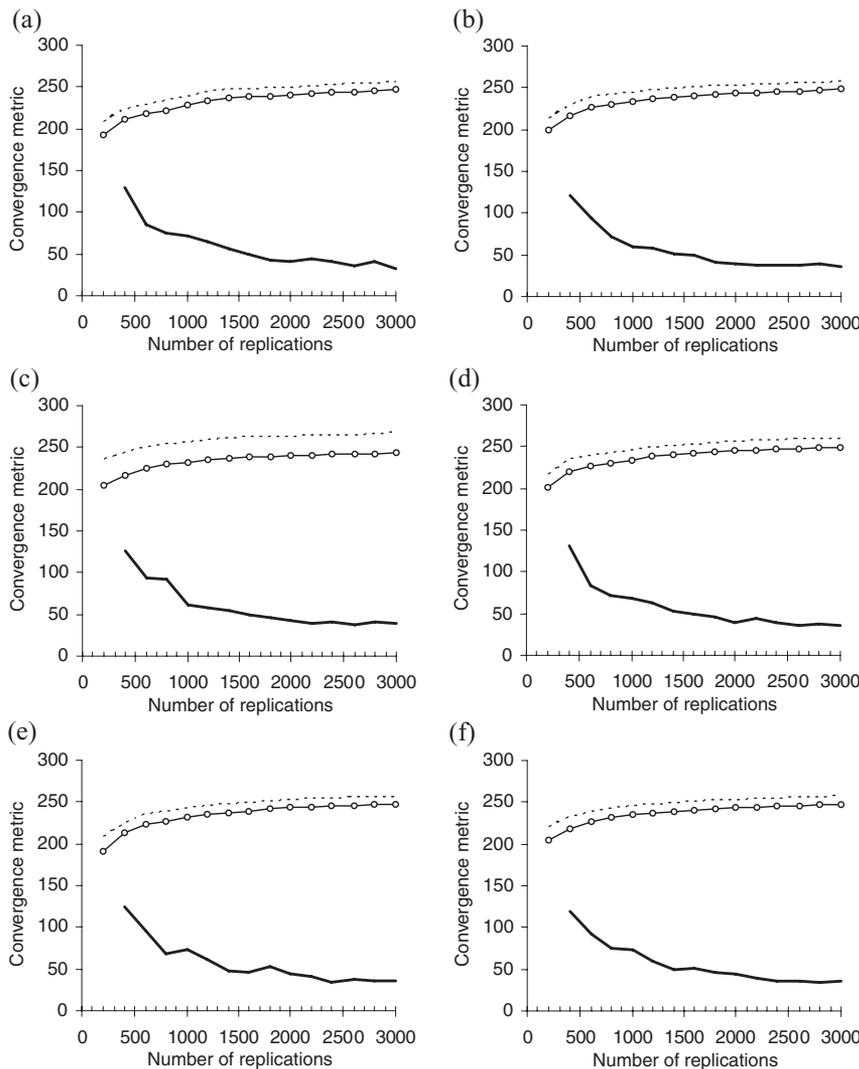
(a)

(b)

(c)

(d)

(e)

(f)

Fig. 1. Convergence metric values versus number of replications, at 40% added parametric uncertainty. Tested parameters: (a) local probabilities of entry at marine ports, $W_{x(t)}$; (b) population carrying capacity, k; (c) maximum annual spread distance, d_{max}; (d) probability of infestation in the nearest adjacent cell, p_0; (e) host susceptibility, s_v; (f) host growth rate, g_v.

- - - - Square root of the total map area with $p < 0.1$ (km)
——— S_{XY} (squared sum of replication-to-replication differences in p values, over ~156,000 map cells)
—○— Square root of the total map area with $\sigma(p) < 0.2$ (km)

(uncertainty) of the output risk estimate, while a ratio value near 0 or much above 1 indicates a noteworthy impact of added parametric uncertainty.

For each sensitivity scenario, we also plotted the regions where adding parameter variation changed the mapped risk estimates considerably. To do so, we divided the baseline risk map into three broad classes, "low," "medium," and "high" risk, corresponding to the p intervals of [0, 0.25],]0.25, 0.75], and]0.75, 1], respectively. We then determined, for each sensitivity scenario, the percentage of map area that shifted from one risk class to another. The shifts from one risk class to another can also be represented in a classified map, which can help identify geo-

graphic locations that exhibited considerable changes in infestation risks, and can also be used to determine what portions of the risk map for each sensitivity scenario remained unchanged despite a given increase in parametric uncertainty.

3. RESULTS

3.1. Baseline Scenario Maps

The map products for the baseline scenario (Fig. 2) illustrate several broad predictions regarding the *S. noctilio* invasion in eastern North America. First, invasion risks (i.e., p; Fig. 2a) are high
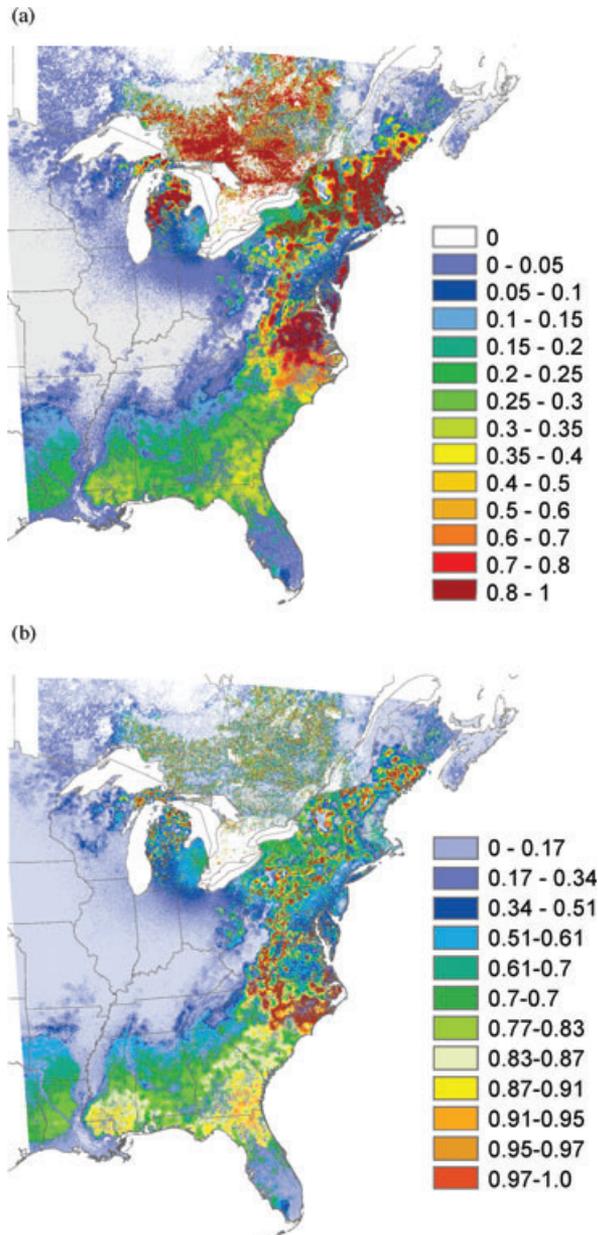
Fig. 2. *S. noctilio* risk maps for the baseline scenario: (a) invasion risk, *p*; (b) variation of the risk values, $\sigma(p)$.

presence. The output uncertainty tends to be high here because the probability of a new *S. noctilio* entry at any port, and its subsequent spread and establishment, is relatively moderate compared with the probability of expansion in northern areas near the existing infestations. Notably, areas of the southeastern United States that are further inland (i.e., noncoastal) typically exhibit low risk and low uncertainty, reflecting less abundant host resources and/or greater distance from possible sources of invaders.

3.2. Uncertainty Ratios

The uncertainty ratio maps show impacts of added parametric uncertainty on the spatial variation of risk estimates across the study area. Fig. 3 shows uncertainty ratio maps for several key parameters at 40% added parametric uncertainty (i.e., the parameters were varied uniformly within ±40% of their baseline value). With respect to the one-parameter-at-a-time sensitivity analyses (Figs. 3(a)–3(c)), the maximum annual spread distance, d_{max} (Fig. 3(a)), exhibited the most significant increases in uncertainty ratios across much of the map area. Notably, high uncertainty ratios occurred in a wide band beyond the leading edge of the estimated invasion front as well as in a few areas within the front (e.g., coastal New England) that were of high risk, yet of low uncertainty, under the baseline scenario. A second parameter, the probability of invasion in the nearest neighboring cell, p_0 (Fig. 3(b)), also exhibited elevated uncertainty ratio values in similar geographic locations, but to a lesser degree. In addition, ratios for p_0 were notably less than 1 in the northwestern portion of our study area. We believe increased parametric uncertainty enabled more invasion nuclei to enter this remote, yet host-rich, area through time, leading to alteration of the invasion risk estimates but partial stabilization of the output uncertainties at a slightly lower level than under the baseline scenario. This same phenomenon occurred with the other parameters (i.e., besides d_{max}). The ratio map for the port entry probabilities parameter, $W_{x(t)}$ (Fig. 3(c)), illustrates another common phenomenon that locations with high uncertainty ratios are generally limited to a small, inland portion of the study area, even in scenarios assuming very high added parametric uncertainty (40%).

Uncertainty ratios for the all-but-one sensitivity scenarios (Figs. 3(d)–3(f)) essentially show the inverse of the one-at-a-time scenarios. When d_{max} (Fig. 3(d)) was the only parameter left fixed at its
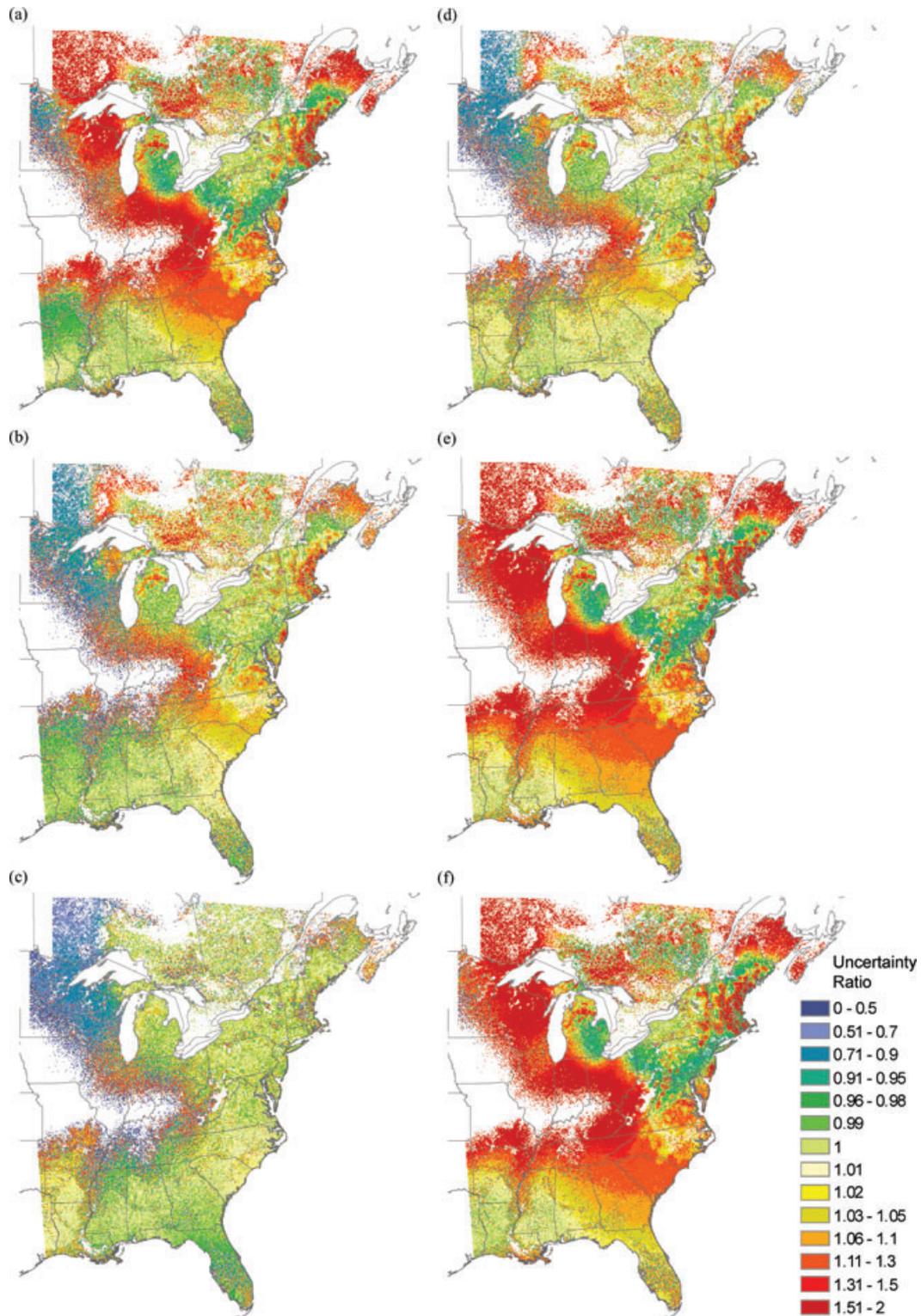
throughout the northeastern United States, southern Ontario, and Quebec and also at the northern end of the southeastern U.S. region. Basically, this depicts the expected path of the invasion over 30 years. Output uncertainty (i.e., $\sigma(p)$; Fig. 2b) is generally highest near the predicted front of the invasion. Beyond the main front, the southeastern United States contains extensive areas of medium-level risk near the Atlantic and Gulf coasts (i.e., near possible ports of entry), throughout which there is a substantial host

Fig. 3. Maps of uncertainty ratios generated through sensitivity analyses. One-parameter-at-a-time sensitivity analysis scenarios: (a) d_{max}, (b) p_0, (c) $W_{x_{(t)}}$. All-but-one (i.e., single parameter left fixed) scenarios: (d) fixed d_{max}, (e) fixed k, (f) fixed g_v. Scenarios at 40% added parametric uncertainty are shown. For any map cell, the uncertainty ratio is the $\sigma(p)$ value for the sensitivity scenario of interest divided by the $\sigma(p)$ value from the baseline scenario.
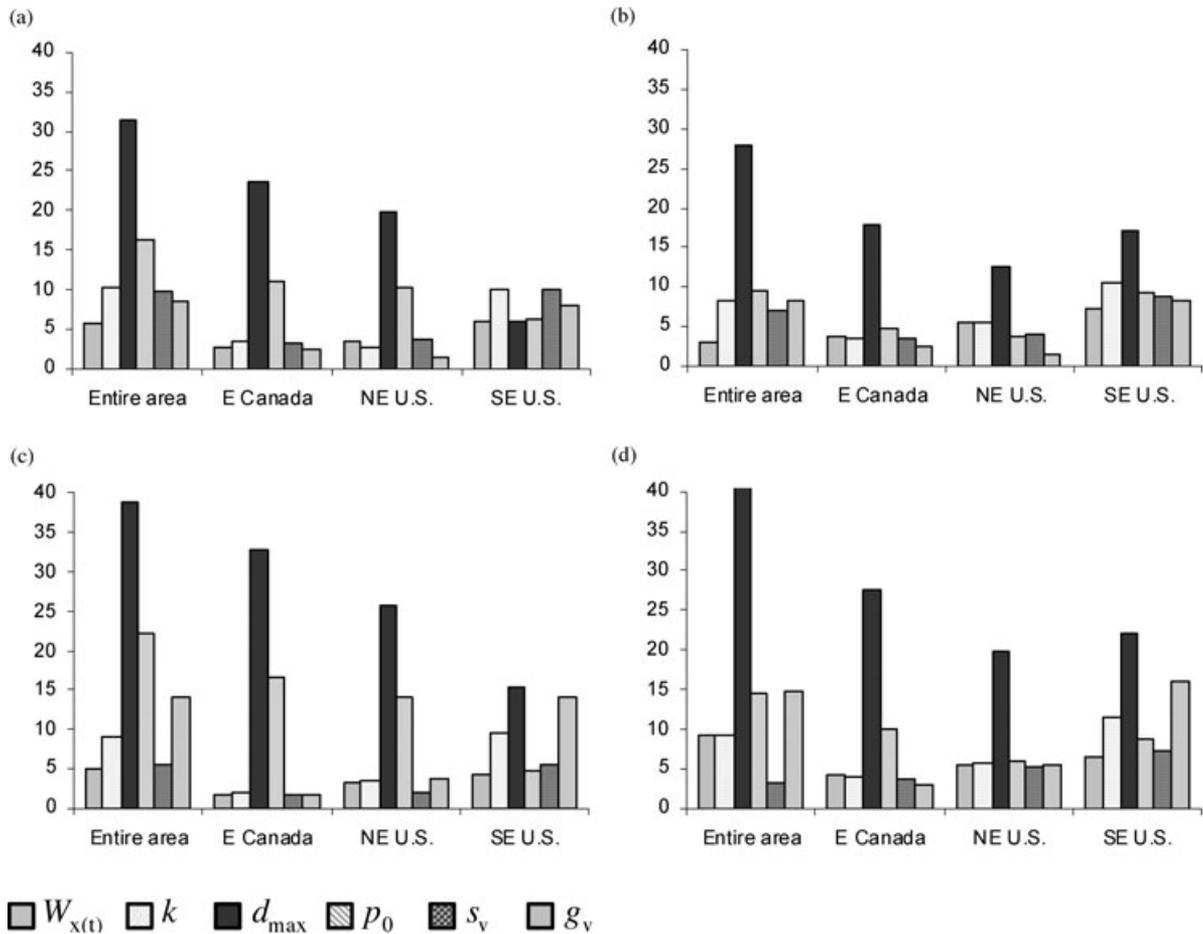
Fig. 4. Regional summaries of the S_{XY} metric for the sensitivity analyses. Results from one-parameter-at-a-time sensitivity analyses are presented in two variability increments: (a) S_{XY} for p at 25% added parametric uncertainty, (b) for $\sigma(p)$ at 25%, (c) for p at 40%, (d) for $\sigma(p)$ at 40% added parametric uncertainty.

baseline value, and all other parameters were varied uniformly within a $\pm40\%$ bound, the uncertainty ratios were low to moderate throughout nearly the entire study area. However, when any other single parameter was left fixed, such as the population carrying capacity, k (Fig. 3(e)), or the host growth rate, g_v (Fig. 3(f)), substantial increases in uncertainty ratio values were observable across a large portion of the study area. These results further suggest that d_{max} had the most influence on the model outputs, including the variation of the risk estimates.

3.3. Regional Summaries

Fig. 4 shows S_{XY}, the sum of the cumulative differences between the sensitivity scenario's p and $\sigma(p)$ maps and the corresponding baseline projections of p and $\sigma(p)$. The results are shown at two levels of added parametric uncertainty, 25% and 40%. In this case, X denotes the sensitivity scenario and Y is the scenario using the baseline parameter values. When we calculated S_{XY} for the entire study area, and whether we did so based on p or $\sigma(p)$, the results echoed the uncertainty ratio maps: d_{max} was the most important model parameter by a substantial margin. The graphs of S_{XY} for the risk of invasion p (Figs. 4(a) and (c)) further suggest that p_0 was the second-most sensitive parameter when including the entire study area, but at a noticeably lower level of importance. A third parameter, g_v, also exhibited low-to-moderate sensitivity, but this was only distinguishable at 40% added uncertainty (Figs. 4(c) and (d)).

The S_{XY} values for the eastern Canada and northeastern U.S. regions similarly indicated d_{max} as the most important parameter and p_0 as more

sensitive than the other four tested parameters. In contrast, the results for the southeastern U.S. region suggest relatively lower importance for d_{max} and that, under a high level of added uncertainty (Figs. 4(c) and (d)), g_v was nearly as important. This may be partially explained by the fact that the southeastern United States is farthest from the existing infested locations, so successful invasions may only develop from new entries, which are relatively rare and may not occur until late in the 30-year time frame. Given the latter point, it makes sense in this situation that a parameter governing the abundance of the suscepti-ble host resource would influence the invasion model nearly as much as one shaping the maximum rate of spread.

3.4. Shifts in Risk Classes

Table I shows the percentages of map area that shifted from one risk class to another in the one-parameter-at-a-time sensitivity analyses. The results are displayed for sensitivity scenarios completed at low (10%), moderate (25%), and high (40%) levels of added parametric uncertainty. At 10% added un-certainty, the scenarios displayed generally modest shifts in risk classes (less than 5% of the map area relative to the baseline scenario), although one pa-rameter, the local probability of entry, $W_{x(t)}$, exhib-ited a relatively large shift (8.3% of the map area between the medium- and low-risk classes). We be-lieve this reflects the phenomenon, noted earlier, of added variability in a parameter causing more inva-sion nuclei to enter geographically remote portions of the study area through time, altering invasion risk but stabilizing output uncertainty, $\sigma(p)$, to a lim-ited degree. We interpret similarly the shifts between medium and low risk for $W_{x(t)}$ (8.1% of map area) and between high and medium risk for p_0 (8.1%) at 40% added uncertainty; indeed, this interpreta-tion likely applies to many of the observed changes in risk caused by added parametric uncertainty. Re-

Table I. The Percentage of Map Area Shifting from One Risk Class to Another When Varying One Parameter at a Time Within Three Different Symmetric Uniform Ranges: ±10%, ±25%, and ±40%; Percentages Are Relative to the Class Area Totals for the Baseline Scenario

Shift in Risk Class	Model Parameter					
	$W_{x(t)}$	k	d_{max}	p_0	s_v	g_v
10% added parametric uncertainty						
Low→medium*	0.5	4.3	3.0	1.0	1.3	1.7
Medium→low	8.3	1.2	3.5	5.4	4.4	2.6
High→medium	1.0	0.9	4.9	1.1	1.0	0.9
Medium→high	0.7	0.6	0.2	0.6	0.5	0.8
25% added parametric uncertainty						
Low→medium	2.2	2.8	3.5	2.3	2.6	2.5
Medium→low	1.7	1.3	6.6	2.0	1.6	3.7
High→medium	1.3	1.0	17.4	4.6	1.1	0.9
Medium→high	0.6	0.7	0.1	0.2	0.7	0.6
40% added parametric uncertainty						
Low→medium	0.6	3.7	4.4	1.4	2.1	5.8
Medium→low	8.1	2.2	5.7	5.5	3.5	1.1
High→medium	1.2	1.3	27.7	8.1	1.1	1.1
Medium→high	0.6	0.6	0.0	0.1	0.6	0.6

*Low risk: $p < 0.25$, medium risk: $0.25 \leq p \leq 0.75$, high risk: $p > 0.75$.

gardless, Table I also shows that d_{max} scenarios ex-hibited larger map area shifts (from high to medium risk) at 25% and 40% added uncertainty than any other parameter. The results for d_{max} from all one-at-a-time sensitivity analysis scenarios (Table II) show a 9.8% map area shift between high and medium risk at 15% added uncertainty. This is larger than any shift observed, at any variability bound increment, with respect to the other five parameters. Furthermore, there was also a large shift between medium and low risk (8.1% of map area) at 15% added parametric un-certainty for d_{max}.

Fig. 5 depicts the shift from one risk class to an-other for eastern North America for the scenarios with 15% and 50% added uncertainty in d_{max}. At 15% added uncertainty (Fig. 5(a)), much of the area

Shift in Risk Class	Uniform Variation of d_{max}, Percentage of the Baseline Value								
	±5%	±10%	±15%	±20%	±25%	±30%	±35%	±40%	±50%
Low→medium*	1.6	3.0	2.9	3.5	3.5	3.4	4.1	4.4	6.4
Medium→low	3.8	3.5	8.1	7.4	6.6	5.1	4.8	5.7	7.8
High→medium	3.4	4.9	9.8	12.1	17.4	20.6	25.2	27.7	34.9
Medium→high (×10)	2.8	2.2	1.3	1.1	0.8	0.8	0.4	0.3	0.3

Table II. The Percentage of Total Map Area Shifting from One Risk Class to Another When Varying Only the d_{max} Parameter; Reported Percentages Are Relative to the Class Area Totals for the Baseline Scenario
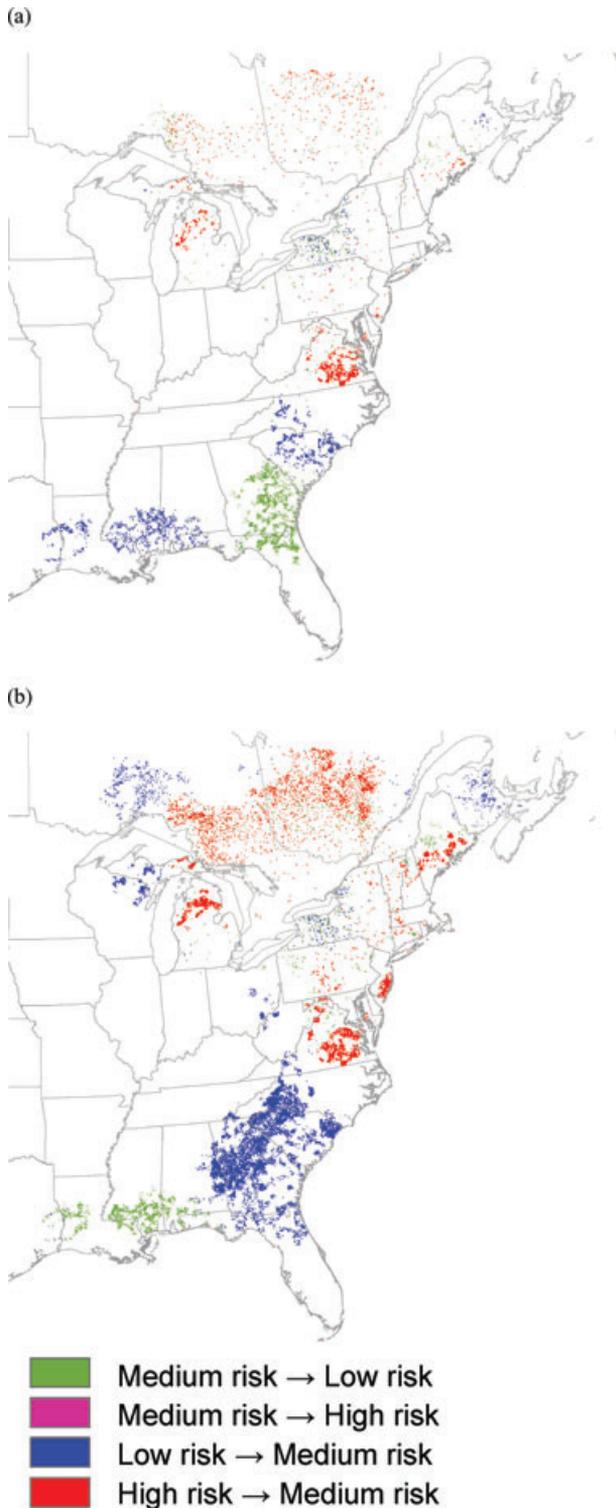
*Low risk: $p < 0.25$, medium risk: $0.25 \leq p \leq 0.75$, high risk: $p > 0.75$.

(a)

(b)

■ Medium risk → Low risk
■ Medium risk → High risk
■ Low risk → Medium risk
■ High risk → Medium risk

Fig. 5. Geographic distribution of the shifts in predicted risk classes due to increased uncertainty in the d_{max} parameter: (a) 15% added uncertainty in d_{max}, (b) 50% added uncertainty in d_{max}. White areas delineate no changes in risk class. Risk classes: low risk, $p < 0.25$; medium risk, $0.25 \leq p \leq 0.75$; high risk, $p > 0.75$.

within the main 30-year invasion front (see Fig. 1) did not experience a shift in risk class, although there were clusters of cells with high-to-medium risk shifts near the southern and northern extents of the front. The risk class shifts in the southeastern United States were mostly limited to coastal areas and reflect a complex relationship between new *S. noctilio* entries at the region's marine ports and their pattern of subsequent expansion into host-rich areas under a variable d_{max}. Similar trends appeared under 50% added parametric uncertainty (Fig. 5(b)), although more map cells were affected. Nonetheless, even at this high level of added uncertainty in d_{max}, large areas both within and beyond the main invasion front displayed no change in risk class.

4. DISCUSSION

Three major points emerge from this analysis. First, the sensitivity analyses revealed that the maximum annual spread distance, d_{max}, was the most influential component in our integrated risk model. This has important ramifications for pest risk modeling. Foremost, for an invasion occurring across a moderate-length time frame, the long-distance component of the invasion will substantially determine its progress in any given year. Moreover, the parameter that we identified as the next most sensitive, p_0, significantly influences local dispersal. Importantly, the d_{max} value combines with the local dispersal probability represented by p_0 to affect the overall shape of the dispersal kernel. Thus, it appears that uncertainties associated with the spread component of our risk model generally have the greatest influence on the reliability of the output risk map. For *S. noctilio*, this may be partially explained by the fact that the insect has already established a significant presence in our study area, and thus the potential risks from spread of existing populations outweigh the threats from potential new entries. This is less true in the southeastern United States, which is farthest from the existing infestations; in this region, factors related to successful establishment (e.g., the host growth rate, g_v, and the carrying capacity, k) also become fairly important. In any case, the generally high sensitivity of model predictions to the dispersal parameters is not surprising.[70–72] Still, it should be acknowledged that long-distance and human-mediated dispersal are poorly understood phenomena;[73–76] indeed, this lack of knowledge has been recognized as a major concern in many other studies of

invasive species.[70,72,74,77,78] We believe that the currently limited understanding about the dispersal of invasive pests is a significant challenge for pest risk assessment activities and so should be a focus of modeling research efforts.

Our study employed an arbitrary designation of the low-, medium-, and high-risk classes. This sacrifices some of the precision in the probabilistic estimates of p, but doing so offers a simple and illustrative way to quantify the influence of added parametric uncertainty on the stability of the output risk map. Our analysis of the shifts between risk classes emphasizes the importance of d_{max}, but it also reveals where the risk map begins to change in a manner that may compromise its utility for decision support. In our view, either a decrease or an increase in the predicted risk class due to uncertainty could be problematic. A decrease means that adequate resources to combat an invader may not be directed to the area of interest because the true risk may have been underpredicted there. Conversely, an increase, or overprediction, of the true risk could lead to too many resources being devoted to a particular area of interest at the expense of others. This, however, raises the issue of appropriate thresholds for declaring that a risk map is no longer stable. For our *S. noctilio* example, added uncertainty in d_{max} resulted in map area shifts, between high and medium risk, that were larger than any shifts seen with the other tested parameters, at any level of variability. The first of these comparatively large shifts (i.e., nearly 10% relative to the baseline) appeared at 15% added uncertainty for d_{max}. This suggests that somewhere between 10% and 15% added uncertainty in d_{max}, the *S. noctilio* risk map experienced a noticeable decline in overall stability.

Nonetheless, and this is our third major point, many areas of the risk map were unchanged despite added variation in the parameter values. This was even true with 50% added parametric uncertainty. Most obviously, areas close to the existing infestations, in general, retained their risk class, which is not surprising because even with a substantial increase in d_{max} variation, these areas are still likely to experience invasion by the end of the forecast horizon. It also seems reasonable to assume that many inland areas in the southeastern United States are unlikely to be invaded within the 30-year forecast horizon without human-assisted dispersal, even if the dispersal capability of *S. noctilio* is substantially underestimated by the current model.

4.1. Implications of the Approach

The approach presented here has a fairly traditional foundation, relying on established Monte Carlo techniques for sensitivity analysis[22,24] to evaluate uncertainty for a particular, spatially explicit risk modeling context. We have depicted the conservative premise that the most important drivers of a new pest's invasion will likely be poorly understood. Even if they are adequately specified, our approach permits us to evaluate whether uncertainty in any of these drivers will have meaningful consequences for the mapped risk estimates. In addition, determining which of the risk model's parameters contributes the most to its overall uncertainty helps to identify where parameter refinements may be possible (e.g., through field data collection).[69] Notably, the approach accommodates rapid updates should new invasion loci be detected, which is an important consideration for adaptive management of invasive pests.

Another advance of the methodology presented here is the development of metrics for quantifying the impact of uncertainty in risk map products. The study illustrates how these metrics (e.g., S_{XY} and the shifts in risk classes) can be used to sketch out a horizon of parameter variation beyond which the output map loses its stability. However, the method may not be applicable in cases in which information for parameterizing the risk model is severely limited, as it requires at least approximate knowledge of the baseline parameter values. We believe that such cases of severe uncertainty necessitate a different approach that does not rely on a probabilistic representation of the structure of uncertainty, such as the info-gap framework.[35]

The study had several limitations that must be recognized. First, the analysis is computationally intensive and included more than 100 sensitivity analysis scenarios, each requiring 3,000 individual model replications. Sampling techniques such as the Latin hypercube sampling[44,79] could reduce the number of replications (and thus the computation time). Second, we only examined six parameters for this study. Our choices were guided by our familiarity with the model and also preliminary tests, but it would be straightforward to apply the approach to other less critical parameters. The study also did not explore uncertainties in the geographic inputs (such as pine host distribution or the locations of marine ports). The input data may contain spatial uncertainties linked to certain types of heterogeneities and landscape features (such as patches or corridors).

Technically, our approach can be applied to analyze these geographic uncertainties, but would require generating series of maps with randomized realizations of spatial heterogeneities and then sampling these maps in a sensitivity analysis. This topic warrants further investigation.

Third, this study did not examine uncertainties associated with model functional structure and formulation. There are ensemble or multimodel approaches that combine the results of several different models into a unified spectrum of uncertainty.[19,80] Our approach can be adapted to explore this issue, but would require significant effort in incorporating other models and still would not guarantee that all plausible models had been included.[19] More critically, there is some danger of including inappropriately formulated models in such an exercise.[81] Overall, the presented modeling framework is consistent with the general understanding of the dynamics of biological invasions,[5] and the findings can be used to guide further modeling efforts. Indeed, in future work, we will focus on reformulating the risk model to accommodate the possibility of human-mediated dispersal, which is acknowledged as a poorly characterized, yet highly important, factor for a growing number of pests.[82–84]

5. CONCLUSIONS

The typical lack of knowledge about recently recognized invasive pests and related uncertainties of pest risk models can limit the utility of risk mapping efforts. Our study explored certain aspects of this problem, most notably how uncertainty in a risk model's numeric assumptions may change a risk map and thus its reliability as a decision support tool. Sensitivity analysis of a *Sirex noctilio* risk map and underlying risk mapping model for eastern North America identified the maximum annual spread distance as the most critical model assumption affecting the estimates of risk. The risk map begins to lose some of its stability when the uncertainties about this parameter reach 15% of its nominal value, emphasizing the importance of the long-distance dispersal component in the overall model formulation. The study also outlines an approach in which sensitivity analysis is used to identify geographical hotspots in risk maps that may be affected by uncertainties in key assumptions about an invader. We believe that detailed consideration of uncertainty and application of sensitivity analyses in a manner such as described here should be standard procedures in pest risk mapping, especially because they will indicate ways to ultimately improve the accuracy and utility of these efforts.

REFERENCES

1. Pimentel D, McNair S, Janecka J, Wightman J, Simmonds C, O'Connell C, Wong E, Russel L, Zern J, Aquino T, Tsomondo T. Economic and environmental threats of alien plant, animal, and microbe invasions. Agriculture, Ecosystems and Environment, 2001; 84:1–20.
2. Perrings C, Dehnen-Schmutz K, Touza J, Williamson M. How to manage biological invasions under globalization. Trends in Ecology & Evolution, 2005; 20(5):212–215.
3. Westphal MI, Browne M, MacKinnon K, Noble I. The link between international trade and the global distribution of invasive alien species. Biological Invasions, 2008; 10:391–398.
4. Kolar CS, Lodge DM. Progress in invasion biology: Predicting invaders. Trends in Ecology & Evolution, 2001; 16(4):199–204.
5. Drake JM. Risk analysis for invasive species and emerging infectious diseases: Concepts and applications. American Midland Naturalist, 2005; 153:4–19.
6. Sanders NJ, Gotelli NJ, Heller NE, Gordon DE. Community disassembly by an invasive species. Proceedings of the National Academy of Sciences of the United States of America, 2003; 100(5):2474–2477.
7. Davis MA. Biotic globalization: Does competition from introduced species threaten biodiversity? BioScience, 2003; 53(5):481–489.
8. Wilcove DS, Rothstein D, Dubow J, Phillips A, Losos E. Quantifying threats to imperiled species in the United States. BioScience, 1998; 48(8):607–615.
9. Andersen MC, Adams H, Hope B, Powell M. Risk analysis for invasive species: General framework and research needs. Risk Analysis, 2004; 24(4):893–900.
10. Baker R, Cannon R, Bartlett P, Barker I. Novel strategies for assessing and managing the risks posed by invasive alien species to global crop production and biodiversity. Annals of Applied Biology, 2005; 146:177–191.
11. Simberloff D. The politics of assessing risk for biological invasions: The USA as a case study. Trends in Ecology & Evolution, 2005; 20(5):216–222.
12. Andersen MC, Adams H, Hope B, Powell M. Risk assessment for invasive species. Risk Analysis, 2004; 24(4):787–793.
13. Mehta SV, Haight RG, Homans FR, Polasky S, Venette RC. Optimal detection and control strategies for invasive species management. Ecological Economics, 2007; 62:237–245.

14. Woodbury PB. Dos and don'ts of spatially explicit ecological risk assessments. Environmental Toxicology and Chemistry, 2003; 22(5):977–982.

15. Foxcroft LC, Rouget M, Richardson DM. Risk assessment of riparian plant invasions into protected areas. Conservation Biology, 2007; 21(2):412–421.

16. Andrews CJ, Hassenzahl DM, Johnson BB. Accommodating uncertainty in comparative risk. Risk Analysis, 2004; 24(5):1323–1335.

17. Baudrit C, Couso I, Dubois D. Joint propagation of probability and possibility in risk analysis: Towards a formal framework. International Journal of Approximate Reasoning, 2007; 45:82–105.

18. Elith J, Burgman MA, Regan HM. Mapping epistemic uncertainties and vague concepts in predictions of species distribution. Ecological Modelling, 2002; 157:313–329.

19. Refsgaard JC, Van Der Sluijs JP, Højberg AL, Vanrolleghem PA. Uncertainty in the environmental modelling process—A framework and guidance. Environmental Modelling & Software, 2007; 22:1543–1556.

20. Regan HM, Colyvan M, Burgman MA. A taxonomy and treatment of uncertainty for ecology and conservation biology. Ecological Applications, 2002; 12(2):618–628.

21. Walker WE, Harramoës P, Rotmans J, Van Der Sluijs JP, van Asselt MBA, Janssen P, Krayer von Krauss MP. Defining uncertainty—A conceptual basis for uncertainty management in model-based decision support. Integrated Assessment, 2003; 4(1):5–17.

22. Li H, Wu J. Uncertainty analysis in ecological studies: An overview. Chapter 3 in Wu J, Jones KB, Li H, Loucks OL (eds). Scaling and Uncertainty Analysis in Ecology: Methods and Applications. Dordrecht, The Netherlands: Springer, 2006.

23. Ades AE, Lu G. Correlations between parameters in risk models: Estimation and propagation of uncertainty by Markov chain Monte Carlo. Risk Analysis, 2003; 23(6):1165–1172.

24. Morgan MG, Henrion M. Uncertainty: A Guide to Dealing with Uncertainty in Quantitative Risk and Policy Analysis. New York: Cambridge University Press, 1990.

25. Regan HM, Akçakaya HR, Ferson S, Root KV, Carroll S, Ginzburg LR. Treatments of uncertainty and variability in ecological risk assessment of single-species populations. Human and Ecological Risk Assessment, 2003; 9(4):889–906.

26. Cook A, Marion G, Butler A, Gibson G. Bayesian inference for the spatio-temporal invasion of alien species. Bulletin of Mathematical Biology, 2007; 69:2005–2025.

27. Lodge DM, Williams S, MacIsaac HJ, Hayes KR, Leung B, Riechard S, Mack RN, Moyle PB, Smith M, Andow DA, Carlton JT, McMichael A. Biological invasions: Recommendations for U.S. policy and management. Ecological Applications, 2006; 16(6):2035–2054.

28. Agumya A, Hunter GJ. Responding to the consequences of uncertainty in geographical data. International Journal of Geographical Information Science, 2002; 16(5):405–417.

29. Crosetto M, Tarantola S. Uncertainty and sensitivity analysis: Tools for GIS-based model implementation. International Journal of Geographical Information Science, 2001; 15(5):415–437.

30. Crosetto M, Tarantola S, Saltelli A. Sensitivity and uncertainty analysis in spatial modelling based on GIS. Agriculture, Ecosystems and Environment, 2000; 81:71–79.

31. Foody GM. Uncertainty, knowledge discovery and data mining in GIS. Progress in Physical Geography, 2003; 27(1):113–121.

32. Karssenberg D, De Jong K. Dynamic environmental modelling in GIS: 2. Modelling error propagation. International Journal of Geographical Information Science, 2005; 19(6):623–637.

33. Burgman MA, Breininger DR, Duncan BW, Ferson S. Setting reliability bounds on habitat suitability indices. Ecological Applications, 2001; 11(1):70–78.

34. Sikder IU, Mal-Sarkar S, Mal TK. Knowledge-based risk assessment under uncertainty for species invasion. Risk Analysis, 2005; 26(1):239–252.

35. Ben-Haim Y. Info-Gap Decision Theory: Decisions Under Severe Uncertainty. Amsterdam, The Netherlands: Elsevier Ltd., 2006.

36. Regan HM, Ben-Haim Y, Langford B, Wilson WG, Lundberg P, Andelman SJ, Burgman MA. Robust decision-making under severe uncertainty for conservation management. Ecological Applications, 2005; 15(4):1471–1477.

37. Yemshanov D, Koch FH, McKenney DW, Downing MC, Sapio F. Mapping invasive species risks with stochastic models: A cross-border US-Canada application for *Sirex noctilio* Fabricius. Risk Analysis, 2009; 29:868–884.

38. Carnegie AJ, Matzuki M, Haugen DA, Hurley BP, Ahumada R, Klasmer P, Sun J, Iede ET. Predicting the potential distribution of *Sirex noctilio* (Hymenoptera: Siricidae), a significant exotic pest of *Pinus* plantations. Annals of Forest Science, 2006; 63:119–128.

39. Corley JC, Villacide JM, Bruzzone OA. Spatial dynamics of a *Sirex noctilio* woodwasp population within a pine plantation in Patagonia, Argentina. Entomologia Experimentalis et Applicata, 2007; 125:231–236.

40. Hoebeke ER, Haugen DA, Haack RA. *Sirex noctilio*: Discovery of a Palearctic siricid woodwasp in New York. Newsletter of the Michigan Entomological Society, 2005; 50(1–2):24–25.

41. de Groot P, Nystrom K, Scarr T. Discovery of *Sirex noctilio* (Hymenoptera: Siricidae) in Ontario, Canada. Great Lakes Entomologist, 2006; 39:49–53.

42. Rossi RE, Borth PW, Tollefson JJ. Stochastic simulation for characterizing ecological spatial patterns and appraising risk. Ecological Applications, 1993; 3(4):719–735.

43. Rafoss T. Spatial stochastic simulation offers potential as a quantitative method for pest risk analysis. Risk Analysis, 2003; 23(4):651–661.

44. Helton JC, Davis FJ. Illustration of sampling-based methods for uncertainty and sensitivity analysis. Risk Analysis, 2002; 22(3):591–622.

45. Yemshanov D, McKenney DW, De Groot P, Haugen DA, Sidders D, Joss B. A bioeconomic approach to assess the impact of a nonnative invasive insect on timber supply and harvests: A case study with *Sirex noctilio* in eastern Canada. Canadian Journal of Forest Research, 2009; 39(1):154–168.

46. Yemshanov D, McKenney DW, Fraleigh S, D'Eon S. An integrated spatial assessment of the investment potential of three species in southern Ontario, Canada inclusive of carbon benefits. Forest Policy and Economics, 2007; 10:48–59.

47. Gibson GJ, Austin EJ. Fitting and testing stochastic models with application in plant epidemiology. Plant Pathology, 1996; 45:172–184.

48. Fuentes MA, Kuperman MN. Cellular automata and epidemiological models with spatial dependence. Physica A, 1999; 237:471–486.

49. Haack RA. Exotic bark- and wood-boring Coleoptera in the United States: Recent establishments and interceptions. Canadian Journal of Forest Research, 2006; 36:269–288.

50. Bartell SM, Nair SK. Establishment risks for invasive species. Risk Analysis, 2003; 24(4):833–845.

51. Herborg L-M, Jerde CL, Lodge DM, Ruiz GM, MacIsaac HJ. Predicting invasion risk using measures of introduction effort and environmental niche models. Ecological Applications, 2007; 17(3):663–674.

52. Statistics Canada. Merchandise imports and exports, by major groups and principal trading areas for all countries, annual (dollars), 1971 to 2007 - CANSIM database table no. 228-0003,

2008. Available at: http://cansim2.statcan.ca, Accessed on June 15, 2008.

53. U.S. Census Bureau. U.S. trade in goods—Balance of payments (bop) basis vs. census basis, 2008. Available at: http://www.census.gov/foreign-trade/statistics/historical/goods.txt, Accessed on October 15, 2008.

54. FAO-IPPC. Guidelines for Regulating Wood Packaging Material in International Trade, International Standards for Phytosanitary Measures No. 15 (Revised). Rome, Italy: United Nations Food and Agriculture Organization (FAO), International Plant Protection Convention (IPPC), 2006.

55. Statistics Canada. Shipping in Canada 2000, catalogue no. 54-205-XIE, 2003. Available at: http://www.statcan.ca/english/freepub/54-205-XIE/0000054-205-XIE.pdf, Accessed on April 30, 2008.

56. Statistics Canada. Shipping in Canada 2001, catalogue no. 54-205-XIE, 2003. Available at: http://www.statcan.ca/english/freepub/54-205-XIE/0000154-205-XIE.pdf, Accessed on April 30, 2008.

57. Statistics Canada. Shipping in Canada 2002, catalogue no. 54-205-XIE, 2004. Available at: http://www.statcan.ca/english/freepub/54-205-XIE/0000254-205-XIE.pdf, Accessed on April 30, 2008.

58. Statistics Canada. Shipping in Canada 2003, catalogue no. 54-205-XIE, 2005. Available at: http://www.statcan.ca/english/freepub/54-205-XIE/0000354-205-XIE.pdf, Accessed on April 30, 2008.

59. Statistics Canada. Shipping in Canada 2004, catalogue no. 54-205-XIE, 2007. Available at: http://www.statcan.ca/english/freepub/54-205-XIE/0000454-205-XIE.pdf, Accessed on April 30, 2008.

60. U.S. Army Corps of Engineers Navigation Data Center. U.S. waterway data, foreign cargo inbound and outbound, 2007. Available at: http://www.iwr.usace.army.mil/ndc/db/foreign/data/, Accessed on August 12, 2008.

61. Sharov AA, Liebhold AM. Model of slowing the spread of gypsy moth (Lepidoptera: Lymantriidae) with a barrier zone. Ecological Applications, 1998; 8(4):1170–1179.

62. Villacide JM, Corley JC. Parasitism and dispersal potential of *Sirex noctilio*: Implications for biological control. Agricultural and Forest Entomology, 2008; 10:341–345.

63. USDA Forest Service Forest Health Technology Enterprise Team (FHTET). Sirex woodwasp (*Sirex noctilio*)—Host species susceptibility, 2007. Available at: http://www.fs.fed.us/foresthealth/technology/pdfs/host_species_susceptibility.pdf, Accessed on August 12, 2008.

64. Gillis MD. Canada's national forest inventory, responding to current information needs. Environmental Monitoring and Assessment, 2001; 67:121–129.

65. Reams GA, Smith WD, Hansen MH, Bechtold WA, Roesch FA, Moisen GG. The forest inventory and analysis sampling frame. Chapter 2 in Bechtold WA, Patterson PL (eds). The Enhanced Forest Inventory and Analysis Program—National Sampling Design and Estimation Procedures. General Technical Report SRS-80. Asheville, NC: USDA Forest Service, Southern Research Station, 2005.

66. Ung C-H, Bernier PY, Guo XJ, Lambert M-C. A simple growth and yield model for assessing changes in standing volume across Canada's forests. Forestry Chronicle, 2009; 85:57–64.

67. Dixon GE, comp. Essential FVS: A User's Guide to the Forest Vegetation Simulator. Internal Report. Fort Collins, CO: U.S. Department of Agriculture, Forest Service, Forest Management Service Center. (Last revised April 7, 2008.) Available at: http://www.fs.fed.us/fmsc/ftp/fvs/docs/gtr/EssentialFVS.pdf, 2002.

68. Johnson CJ, Gillingham MP. Mapping uncertainty: Sensitivity of wildlife habitat ratings to expert opinion. Journal of Applied Ecology, 2004; 41:1032–1041.

69. Cariboni J, Gatelli D, Liska R, Saltelli A. The role of sensitivity analysis in ecological modelling. Ecological Modelling, 2007; 203:167–182.

70. Clark JS, Fastie C, Hurtt G, Jackson ST, Johnson C, King GA, Lewis M, Lynch J, Pacala S, Prentice C, Schupp EW, Webb T, Wyckoff P. Reid's paradox of rapid plant migration: Dispersal theory and interpretation of paleoecological records. BioScience, 1998; 48(1):13–24.

71. Kot M, Lewis MA, Van Den Driessche P. Dispersal data and the spread of invading organisms. Ecology, 1996; 77(7):2027–2042.

72. Neubert MG, Caswell H. Demography and dispersal: Calculation and sensitivity analysis of invasion speed for structured populations. Ecology, 2000; 81(6):1613–1628.

73. Andow DA, Kareiva PM, Levin SA, Okubo A. Spread of invading organisms: Patterns of spread. Chapter 11 in Kim KC, McPheron BA (eds). Evolution of Insect Pests: Patterns of Variation. New York: Wiley, 1993.

74. BenDor TK, Metcalf SS, Fontenot LE, Sangunett B, Hannon B. Modeling the spread of the emerald ash borer. Ecological Modelling, 2006; 197:221–236.

75. Hastings A, Cuddington K, Davies KF, Dugaw CJ, Elmendorf S, Freestone A, Harrison S, Holland M, Lambrinos J, Malvadkar U, Melbourne BA, Moore K, Taylor C, Thomson D. The spatial spread of invasions: New developments in theory and evidence. Ecology Letters, 2005; 8:91–101.

76. Hovestadt T, Messner S, Poethke HJ. Evolution of reduced dispersal mortality and "fat-tailed" dispersal kernels in autocorrelated landscapes. Proceedings of the Royal Society of London B, 2001; 268:385–391.

77. Bossenbroek JM, Kraft CE, Nekola JC. Prediction of long-distance dispersal using gravity models: Zebra mussel invasion of inland lakes. Ecological Applications, 2001; 11(6):1778–1788.

78. Higgins SI, Richardson DM, Cowling RM. Validation of a spatial simulation model of a spreading alien plant population. Journal of Applied Ecology, 2001; 38:571–584.

79. Xu C, He HS, Hu Y, Chang Y, Li X, Bu R. Latin hypercube sampling and geostatistical modeling of spatial uncertainty in a spatially explicit forest landscape model simulation. Ecological Modelling, 2005; 185:255–269.

80. Hartley S, Harris R, Lester PJ. Quantifying uncertainty in the potential distribution of an invasive species: Climate and the Argentine ant. Ecology Letters, 2006; 9:1068–1079.

81. Sutherst RW, Bourne AS. Modelling non-equilibrium distributions of invasive species: A tale of two modelling paradigms. Biological Invasions, 2009; 11:1231–1237.

82. Kraus F, Campbell EW. Human-mediated escalation of a formerly eradicable problem: The invasion of Caribbean frogs in the Hawaiian Islands. Biological Invasions, 2002; 4:327–332.

83. Stone GN, Challis RJ, Atkinson RJ, Csóka G, Hayward A, Melika G, Mutun S, Preuss S, Rokas A, Sadeghi E, Schönrogge K. The phylogeographical clade trade: Tracing the impact of human-mediated dispersal on the colonization of northern Europe by the oak gallwasp *Andricus kollari*. Molecular Ecology, 2007; 16:2768–2781.

84. Ward DF, Beggs JR, Clout MN, Harris RJ, O'Connor S. The diversity and origin of exotic ants arriving in New Zealand via human-mediated dispersal. Diversity and Distributions, 2006; 12:601–609.